



Published in final edited form as:

Gastrointest Endosc. 2008 September ; 68(3): 520–527. doi:10.1016/j.gie.2008.02.023.

Biochromoendoscopy: Molecular Imaging with Capsule Endoscopy for Detection of Adenomas of the Gastrointestinal Tract

Howard Zhang, M.D.¹, Douglas Morgan, M.D.¹, Gerald Cecil, PhD², Adam Burkholder, B.S.³, Nicole Ramocki, B.S.⁴, Brooks Scull, B.S.⁴, and P. Kay Lund, PhD⁴

¹Division of Gastroenterology and Hepatology, University of North Carolina at Chapel Hill, Chapel Hill, North Carolina, USA

²Department of Physics and Astronomy, University of North Carolina at Chapel Hill, Chapel Hill, North Carolina, USA

³Department of Biomedical Engineering, University of North Carolina at Chapel Hill, Chapel Hill, North Carolina, USA

⁴Department of Cell and Molecular Physiology, University of North Carolina at Chapel Hill, Chapel Hill, North Carolina, USA

Abstract

Background—Current capsule endoscopy (CE) provides minimally invasive technology for gastrointestinal imaging, but has limited ability to discriminate different polyp types. Near Infrared Fluorescent (NIRF) probes activated by biomarkers upregulated in adenomas (e.g., cathepsin B) are potentially powerful tools to distinguish premalignant or malignant lesions from benign or inflammatory lesions.

Objectives—To examine whether CE can be integrated with NIRF probes to detect adenomas, and whether cathepsin B activated NIRF probes are activated by benign or inflammatory ones.

Design and Setting—Mouse models of adenomas, hyperplastic/lymphoid polyps, and acute or chronic intestinal inflammation were injected intravenously with a cathepsin B activated probe (Prosense™ 680). Dissected intestine was imaged with CE under white or NIRF light. For NIRF, excitation (680 nm), dichroic and emission (700 nm) filters were combined with CE when images were recorded. Prosense™ 680 samples with or without protease were used as positive and negative controls. CE based imaging data was verified using an independent imaging system (Xenogen IVIS system).

Main Outcome Measurements—Proof of principle that CE integrated with NIRF probes can detect and discriminate adenomas from other lesions.

Results—CE based NIRF imaging with Prosense™ 680 readily visualized adenomas, including in the colitis model. NIRF signals of different intensities were detected. Prosense™ 680 was not activated by benign or inflammatory lesions.

Corresponding Author: Brooks Scull, CB#7545, Department of Cell and Molecular Physiology, University of North Carolina at Chapel Hill, Chapel Hill, NC 27599-7545, Phone: 919-966-1490, Fax: 919-966-6927, E-mail: scull@email.unc.edu.

Presentations: Digestive Disease Week, Washington DC, May 23, 2007, Biochromoendoscopy: Capsule Endoscopy with the Cathepsin B Activated Molecular Probe for Imaging Intestinal and Gastric Adenomas

Conflict of Interest Disclosure statement The work in this paper was funded by the National Institutes of Health grant P30 DK 34987 and DK40247. Doug Morgan has participated in clinical trials and speaker's bureau with Given Imaging.

Limitations—Optical filters external to capsule were used.

Conclusions—We demonstrate proof of principle of biochromoendoscopy, CE combined with molecular probes, provides a novel approach that differentiates adenomas from benign polyps and inflammatory lesions.

Keywords

Capsule endoscopy; Near Infrared Fluorescent Imaging; Cathepsin B

INTRODUCTION

Early detection of premalignant and malignant lesions is crucial for the prevention and treatment of gastrointestinal cancers. With the advent of fiberoptic endoscopy, lesions of the upper gastrointestinal (GI) tract and colon can be readily detected. However, the majority of the small intestine remains inaccessible with conventional endoscopy. As with all invasive procedures, fiberoptic endoscopy has finite risks including bleeding, perforation and sedation-associated cardiopulmonary complications.

Capsule endoscopy (CE) is a minimally invasive technology which was originally designed to provide diagnostic imaging of the entire small intestine^{1, 2}. The commercially available endoscopic capsule is composed of a lens, light-emitting diodes (LEDs), digital imager (CMOS chip), battery, and transmitter. Once the capsule is swallowed, white light images are captured and transmitted to a recorder via sensor arrays fastened to the abdomen. Data collected in the recorder can then be downloaded and analyzed as a video. Current indications for CE are evolving and include obscure gastrointestinal hemorrhage, Crohn's disease, and the diagnosis of small bowel polyps or tumors³. There is increasing interest in the use of CE for detection of pathology in esophagus, stomach and colon⁴⁻⁶. However, CE cannot readily classify abnormalities as malignant (adenocarcinoma), premalignant (adenoma), or benign (hyperplastic, lymphoid).

Certain molecular biomarkers, including proteases such as cathepsin B, are up regulated in neoplastic lesions⁷. Synthetic probes activated by these biomarkers, termed "molecular beacons", may be valuable tools for detecting premalignant and malignant lesions⁸⁻¹¹. These probes are intravenously administered and are essentially undetectable in tissues unless locally activated by enzymes that specifically cleave and activate the probe, causing the probe to emit near infrared fluorescence (NIRF)^{12, 13}. *Apc^{Min/+}* mice are a model of adenomatous polyposis of small intestine and colon. In this model, a cathepsin B activatable NIRF probe has been shown to be highly sensitive in the detection of even small adenomas, and to distinguish neoplastic lesions from normal mucosa with high specificity⁹. Prior studies using this probe detected the emitted NIRF by conventional fluorescence microscopy⁹ or by a real-time animal model endoscope equipped with modified near infrared light source, appropriate filters and a charge-coupled device (CCD) camera¹⁴. Like conventional fiberoptic endoscopy, the use of fiberoptic endoscopy in combination with molecular probes is invasive. The potential for distinguishing premalignant lesions from benign polyps and inflammatory lesions using this imaging technology has not been reported.

In our study, we aimed to provide proof of principle that biochromoendoscopy, which combines CE and molecular probe-based imaging technology, can be successfully integrated to detect premalignant lesions. We also aimed to evaluate whether the cathepsin B activated NIRF probe (ProsenseTM 680) can differentiate premalignant from benign polyps and inflammatory lesions. To this end, we compared activation of ProsenseTM 680 by adenomatous polyps, hyperplastic and lymphoid polyps, and acute and chronic inflammatory lesions collected from several

mouse models that have previously been well-characterized for development of these distinct lesion types¹⁵⁻¹⁸.

MATERIALS AND METHODS

Animal Models

A protocol for animal use in this study was approved by the University of North Carolina (UNC) Institutional Animal Care and Use Committee. Mice carrying an inactivating Min mutation in the adenomatous polyposis coli (Apc) gene (*Apc*^{Min/+} mice) were used as a well characterized model of premalignant adenomatous colonic polyps. *Apc*^{Min/+} mice on a C57BL6 background¹⁸ and normal wild type (WT) littermates were purchased from Jackson laboratories and expanded in our facility. For benign lesions we used a *SOCS2-HT/GH-TG* mouse model of combined heterozygous disruption of one allele encoding suppressor of cytokine signaling-2 (SOCS2-HT) and expression of a growth hormone (GH) transgene (GH-TG), or *GH-TG* mice that express the GH transgene but have both SOCS2 alleles intact. We recently showed that *SOCS2-HT/GH-TG*, and to a lesser extent *GH-TG* mice develop spontaneous lymphoid and hyperplastic polyps in the colon which are considered benign lesions with limited potential for progression to adenoma or adenocarcinoma¹⁵. Derivation and characterization of *SOCS2-HT/GH-TG* and *GH-TG* mice on a C57BL6 background were described recently¹⁵. We used wild type (WT) mice treated with sodium dextran sulfate (DSS) as a model of mucosal injury and acute inflammation mediated primarily by macrophages and neutrophils¹⁶. WT mice on the C57BL6 background were given 3% (wt/vol) dextran sulfate sodium (DSS; mol wt, 34,000–45,000) in the drinking water for 5 days¹⁹. The mice were subsequently sacrificed on day 3 and day 10 after the end of DSS treatment, times when we, and others have established that the mice show acute inflammation¹⁶. We used mice homozygous for disruption of both interleukin-10 alleles (interleukin 10 null or *IL-10*^{-/-}) as a model of chronic T cell mediated transmural inflammation that can be accompanied by colitis associated dysplasia or neoplasia¹⁷. *IL-10*^{-/-} mice on a 129SVEv background raised under specific pathogen free conditions were derived from colonies maintained at UNC. The genotypes of all mouse models were confirmed by PCR on DNA isolated from tail clips. Mice were studied between 180 and 240 days of age, times when disease is reliably manifested in all models.

Probe administration, tissue collection, positive and negative controls

Mice were given a cathepsin B activatable probe (Prosense™ 680; VisEN Medical Inc, Woburn, MA), intravenously via tail vein injection at a dose of 2nmol/25 gm wt per animal. Animals were anesthetized and sacrificed 18 hours later and the entire intestine was dissected. The intestine was opened longitudinally and kept moist with phosphate buffered saline and imaged immediately under white light or NIRF. The intestine was subsequently fixed in formalin for 24 hours and preserved in 70% ethanol. Uninjected animals were used as controls. Prosense™ 680 samples added to buffer with and without trypsin, a protease capable of probe activation, served as positive and negative controls. Prosense™ 680 was activated within ten minutes at ambient temperature upon mixing of 10µl 10µM Prosense™ 680, 20µl 5% trypsin (Sigma-Aldrich, St. Louis, MO), and 70µl phosphate buffered saline (PBS). Different concentrations were prepared by serial dilution in PBS.

White Light and NIRF Imaging using CE or conventional imaging

A dedicated light tight imaging chamber was constructed to permit CE based imaging under white light or NIRF (Fig. 1). CE movement through the intestine was simulated with a motorized linear platform mounted with the dissected tissue of interest. The platform and attached tissue were moved at uniform speed across the CE using a stepper motor controlled by a desktop computer running Matlab utilizing a National Instruments USB-6008 data

acquisition device. The CE to tissue distance was constant at 4 cm. Images acquired were transmitted to a recorder via sensor arrays fastened to the outside of the light-tight chamber. Data collected inside the recorder was then downloaded and reviewed in standard fashion. For white light imaging, a CE was suspended above the platform inside the imaging chamber, allowing images of the objects placed on the moving platform to be captured (Fig 1). For NIRF imaging, a similar assembly was used except that an external LED light source was used and a three-component filter set was placed between the tissue and CE (Fig 2). This filter set represents a near-infrared filtering device consisting of excitation (680 nm), dichroic, and emission (700 nm) filters. These filters were situated so that the excitation filter was adjacent to the LED and vertical to the platform. The dichroic filter was 45 degrees to the platform diverting 680 nm light to the tissue, the appropriate wavelength to activate the probe. Activated probe emitted light at 700 nm which can pass through the dichroic filter and the emission filter which was horizontal to the platform and placed immediately in front of the CE. In the NIRF imaging experiments with modified CE, samples were laid out in order from left to right as follows: positive control with activated Prosense™ 680 (AP), negative control with inactive Prosense™ 680 (IP), negative control tissue from uninjected animals (NT), and adenomatous polyps (Ad) dissected from colon of *Apc^{Min/+}* mice (Fig 5, top panel). Correlation was made between the white light and NIRF images by image comparison and by measuring the time elapsed between visualization of the positive control and tissue of interest under white light versus NIRF.

To confirm data obtained with CE and in experiments to test whether Prosense™ 680 discriminated premalignant from hyperplastic or lymphoid polyps, or from acute or chronic inflammation, imaging of samples was also performed with the Xenogen IVIS Imaging System 200 Series and Cy5.5 fluorescent filter set.

RESULTS

NIRF Integrated CE Detects Different Intensity NIRF Signals

Activated Prosense™ 680 (AP) was obtained by mixing 10ml 10mM Prosense™ 680 and 20ml 5% trypsin in 70ml phosphate buffered saline (PBS pH 7.4) at room temperature. Different concentrations were achieved by 1:5 and 1:10 dilution in PBS. The NIRF integrated CE was capable of detecting NIRF signal intensity across this 10 fold probe concentration difference (Fig 3). This provided initial proof of principle that the modified CE system can detect NIRF.

Detection of Adenomatous Polyps in *Apc^{Min/+}* Mice by Modified CE

A white light image of a segment of Prosense™ 680 injected *Apc^{Min/+}* mouse colon containing two adenomatous polyps captured by a conventional CE is shown in Fig 4. The quality of the white-light images obtained using CE in the imaging chamber was excellent. Imaging of the same intestinal segment and polyps with the modified CE detected clear NIRF signals (solid arrows, Fig 5 bottom panels). As expected, NIRF signal was also detected from the positive control (block arrow, Fig 5 bottom panels), but not from the negative controls. Successful NIRF imaging of the adenomas was further confirmed with positioning coordinates from the time record. Using the layout of samples illustrated in the top panel of Fig 5, the time elapsed between NIRF visualization of the activated Prosense™ 680 positive control and visualization of the two adenomatous polyps from the injected *Apc^{Min/+}* mouse (1 minute 18 seconds, Fig 5 bottom panels) was virtually identical to the time elapsed between visualization of these samples under white light (1 minute 16 seconds, Fig 5 middle panels). This provides objective evidence that NIRF signals were indeed emitted from the polyps of Prosense™ 680 injected *Apc^{Min/+}* mouse.

A circular reflection generated by the CE LEDs above the emission filter was visible in the center of the NIRF images. This reflection did not interfere with the visualization of NIRF signals.

In addition to the rounded NIRF signals corresponding to positive control and polyps visualized at the center of the CE viewing field, additional NIRF signals were detected which were artifact from reflection of the external dichroic filter. These signals could easily be distinguished from true NIRF signals and did not confound interpretations when images were viewed as a video. (Video clips are available as supplemental data.)

NIRF Imaging of Murine Colonic Lymphoid and Hyperplastic Polyps

No NIRF signals were detected from the polypoid, non-adenomatous lesions of the large intestines of Prosense™ 680 injected *SOCS2-HT/GH-TG* and *GH-TG* mice by the modified CE (data not shown). Further verification of this finding was carried out by Xenogen IVIS system (Fig 6). The visible polypoid lesions seen in the large intestines of *SOCS2-HT/GH-TG* and *GH-TG* mice were dissected individually and imaged on the same slide with adenomatous polyps from injected *Apc^{Min/+}* mouse and samples of trypsin-activated Prosense™ 680 as positive controls. Only background NIRF signals were detected from these polypoid lesions, while *Apc^{Min/+}* adenomas and activated protease controls yielded strong signals. These polypoid lesions from *SOCS2-HT/GH-TG* and *GH-TG* mice were confirmed to be either lymphoid aggregates or hyperplastic polyps in all cases by histological examination of H&E stained sections of the polyps.

NIRF Imaging of Acute and Chronic Inflammation of Murine Intestines

NIRF signals were not detected using the modified CE in the colon of DSS-treated WT mice or in small intestine or colon of *IL-10^{-/-}* mice (data not shown). Consistent with these findings NIRF images from Xenogen IVIS system showed minimal activation of Prosense™ 680 in the colon of DSS treated mice when referenced with adenomatous polyps from Prosense™ 680 injected *Apc^{Min/+}* mouse and positive control with activated Prosense™ 680 (Fig 7). Similarly, the duodenum, ileum and colon of *IL-10^{-/-}* mice yielded minimal activation of probe. It is established that colon and cecum are major sites of chronic inflammation in the *IL-10^{-/-}* model, and that duodenum can also be involved in older mice as studied here¹⁴. Intriguingly, the cecum of the *IL-10^{-/-}* mice yielded minor background NIRF except for a strong signal in a lesion confirmed as a cecal adenoma (*Cecal Ad*; Fig 7) on histology. This underscores the capability of the probe and modified CE to localize premalignant lesions within a background of chronic inflammation¹⁴.

DISCUSSION

We have demonstrated proof of principle for biochromoendoscopy by integrating “molecular beacons” with NIRF imaging and conventional CE. Our modified CE was capable of detecting NIRF signals emitted from adenomatous polyps in intestines of *Apc^{Min/+}* mice injected with a cathepsin B activatable probe. Importantly, such NIRF signals were specific to the precancerous adenomatous polyps. Benign growths such as hyperplastic polyps or lymphoid aggregates found in similarly treated *SOCS2-HT/GH-TG* or *GH-TG* mice did not emit NIRF signals. In addition, NIRF signals were not observed in inflamed intestine of the DSS acute inflammation model or the *IL-10^{-/-}* chronic inflammation model. Nonetheless, the cathepsin B activated probe did detect an adenoma in the cecum with chronic inflammation of the *IL-10* null mouse model. Together, these findings indicate that the added functionality of the molecular probe combined with CE has the potential to distinguish different types of lesions throughout the GI tract. Future application of biochromoendoscopy in human subjects could

circumvent the diagnostic limitations of existing CE and the invasiveness of conventional endoscopy.

Our results with different doses of activated probe demonstrate that it is possible to detect NIRF signals varying by an order of magnitude. The ability of the integrated CE to detect a difference in NIRF signal intensity is significant since it offers quantification potential. Biomarker-specific signal intensity may reflect the severity of underlying disease processes and may allow a more accurate measurement of the severity or stage of disease process in different subjects. Our current studies used preselected lesions of different types to obtain proof of principle that biochromoendoscopy can be applied to discriminate lesions with differing malignant potential. Future studies could employ the elegant quantitative methods reported by Marten and colleagues⁹, and use CE combined with NIRF to quantify the mean signal intensities and target to background ratio obtained with NIRF probes such as cathepsin B activated Prosense™ 680, or other molecular probes, in our well-characterized mouse models. This would provide quantitative data about the sensitivity and discriminating capabilities of biochromoendoscopy using CE and different molecular probes. Such studies will be best undertaken after further refining of the NIRF integrated CE system.

The quality of the NIRF images from our modified CE integrated with molecular probe is acceptable to show proof of principle, but further improvement can be achieved by reducing the signal artifact of the modified CE. One limitation resulted from the external placement of the filter setup in our prototype, which necessarily meant that tissues were placed at a minimum of 4cm from the CE and external filters. Conventional CE visualizes lesions at close proximity. Various modified CE design options would facilitate direct and close proximity NIRF imaging by CE, to enhance the sensitivity and resolution of the system. For example, the NIRF imaging device can be easily assembled by attaching a round planar filter in front of the lens and illuminating LEDs. This round planar filter would be constructed with a center core emission filter surrounded by an outer donut-shaped excitation filter in proximity to the illuminating LEDs (A, Fig 8). This simpler design would eliminate the need for a dichroic filter, solve signal artifact and reflection problems, and enhance the resolution of NIRF images.

Biochromoendoscopy with integrated CE and molecular imaging could be potentially incorporated into screening programs for colon cancer. Recent studies report that white light CE shows promise in the detection of colonic adenomas compared with conventional fiberoptic colonoscopy^{20, 21}. Our results suggest that modified CE may further enhance the ability to detect and characterize colonic adenomas by visualizing the same lesion under both standard white light image and NIRF image. This may be accomplished, for example, with a modified twin camera capsule (Fig 8), which would be similar to the commercially available esophageal capsule. In addition, because of the specificity of NIRF signals for adenomatous polyps as demonstrated in our study, different types of lesion in the colon could be differentiated by probes activated by specific biomarkers on distinct lesion types, a task difficult to achieve by non-invasive white light based CE. Similarly, biochromoendoscopy has a potentially important role in gastric cancer screening programs in some areas of the world, if the gastric capsule endoscopy is developed and combined with appropriate molecular probes.

Lastly, although we have focused on the use of modified CE with molecular probes for minimally invasive detection and differentiation of premalignant from benign and inflammatory gastrointestinal lesions, this novel approach may have broader applications throughout the GI tract. As more NIRF or other imaging probes for different disease processes are developed^{22, 23}, this technology could potentially allow the detection and differentiation of inflammatory diseases such as Crohn's disease and malignant infiltrative processes such as lymphoma. Biochromoendoscopy may be useful to distinguish inflammatory lesions such as ulcerations caused by Crohn's disease from those induced by medications (e.g. NSAIDs). We

speculate that it may also be useful to identify particular microorganisms in the GI tract if imaging probes specific for the organism are available. The ability to differentiate these very different disease processes in a non-invasive fashion would be invaluable in medical decision making. Lastly, as well as being less invasive than conventional endoscopy, biochromoendoscopy is less resource dependent and could be utilized in populations with limited endoscopy resources.

Acknowledgments

Supported by National Institutes of Health grant P30 DK 34987, DK40247 and DK047769. The authors thank Dr. Yijing Chen (Department of Genetics, University of North Carolina at Chapel Hill, Chapel Hill, NC) for technical assistance.

Grant support: National Institutes of Health grant P30 DK 34987 and DK40247

References

1. Iddan G, Meron G, Glukhovskiy A, et al. Wireless capsule endoscopy. *Nature* 2000;405:417. [PubMed: 10839527]
2. Gong F, Swain P, Mills T. Wireless endoscopy. *Gastrointest Endosc* 2000;51:725–9. [PubMed: 10840312]
3. Schulmann K, Hollerbach S, Kraus K, et al. Feasibility and diagnostic utility of video capsule endoscopy for the detection of small bowel polyps in patients with hereditary polyposis syndromes. *Am J Gastroenterol* 2005;100:27–37. [PubMed: 15654777]
4. Gerson L, Lin OS. Cost-benefit analysis of capsule endoscopy compared with standard upper endoscopy for the detection of Barrett's esophagus. *Clin Gastroenterol Hepatol* 2007;5:319–25. [PubMed: 17368231]
5. Schoofs N, Deviere J, Van Gossum A. PillCam colon capsule endoscopy compared with colonoscopy for colorectal tumor diagnosis: a prospective pilot study. *Endoscopy* 2006;38:971–7. [PubMed: 17058159]
6. Eliakim R, Suissa A, Yassin K, et al. Wireless capsule video endoscopy compared to barium follow-through and computerised tomography in patients with suspected Crohn's disease--final report. *Dig Liver Dis* 2004;36:519–22. [PubMed: 15334771]
7. Koblinski JE, Ahram M, Sloane BF. Unraveling the role of proteases in cancer. *Clin Chim Acta* 2000;291:113–35. [PubMed: 10675719]
8. Massoud TF, Gambhir SS. Molecular imaging in living subjects: seeing fundamental biological processes in a new light. *Genes Dev* 2003;17:545–80. [PubMed: 12629038]
9. Marten K, Bremer C, Khazaie K, et al. Detection of dysplastic intestinal adenomas using enzyme-sensing molecular beacons in mice. *Gastroenterology* 2002;122:406–14. [PubMed: 11832455]
10. Weissleder R, Tung CH, Mahmood U, et al. In vivo imaging of tumors with protease-activated near-infrared fluorescent probes. *Nat Biotechnol* 1999;17:375–8. [PubMed: 10207887]
11. Weissleder R, Ntziachristos V. Shedding light onto live molecular targets. *Nat Med* 2003;9:123–8. [PubMed: 12514725]
12. Campo E, Munoz J, Miquel R, et al. Cathepsin B expression in colorectal carcinomas correlates with tumor progression and shortened patient survival. *Am J Pathol* 1994;145:301–9. [PubMed: 7519824]
13. Emmert-Buck MR, Roth MJ, Zhuang Z, et al. Increased gelatinase A (MMP-2) and cathepsin B activity in invasive tumor regions of human colon cancer samples. *Am J Pathol* 1994;145:1285–90. [PubMed: 7992833]
14. Mahmood U, Weissleder R. Near-infrared optical imaging of proteases in cancer. *Mol Cancer Ther* 2003;2:489–96. [PubMed: 12748311]
15. Michaylira CZ, Ramocki NM, Simmons JG, et al. Haplotype insufficiency for suppressor of cytokine signaling-2 enhances intestinal growth and promotes polyp formation in growth hormone-transgenic mice. *Endocrinology* 2006;147:1632–41. [PubMed: 16410303]

16. Williams KL, Fuller CR, Dieleman LA, et al. Enhanced survival and mucosal repair after dextran sodium sulfate-induced colitis in transgenic mice that overexpress growth hormone. *Gastroenterology* 2001;120:925–37. [PubMed: 11231946]
17. Berg DJ, Zhang J, Weinstock JV, et al. Rapid development of colitis in NSAID-treated IL-10-deficient mice. *Gastroenterology* 2002;123:1527–42. [PubMed: 12404228]
18. Su LK, Kinzler KW, Vogelstein B, et al. Multiple intestinal neoplasia caused by a mutation in the murine homolog of the APC gene. *Science* 1992;256:668–70. [PubMed: 1350108]
19. Savendahl L, Underwood LE, Haldeman KM, et al. Fasting prevents experimental murine colitis produced by dextran sulfate sodium and decreases interleukin-1 beta and insulin-like growth factor I messenger ribonucleic acid. *Endocrinology* 1997;138:734–40. [PubMed: 9003009]
20. Eliakim R, Fireman Z, Gralnek IM, et al. Evaluation of the PillCam Colon capsule in the detection of colonic pathology: results of the first multicenter, prospective, comparative study. *Endoscopy* 2006;38:963–70. [PubMed: 17058158]
21. Schoofs N, Deviere J, Van Gossum A. PillCam Colon capsule endoscopy compared with colonoscopy for colorectal tumor diagnosis: a prospective pilot study. *Endoscopy* 2006;38:971–7. [PubMed: 17058159]
22. Kelly K, Alencar H, Funovics M, et al. Detection of invasive colon cancer using a novel, targeted, library-derived fluorescent peptide. *Cancer Res* 2004;64:6247–51. [PubMed: 15342411]
23. Tung CH. Fluorescent peptide probes for in vivo diagnostic imaging. *Biopolymers* 2004;76:391–403. [PubMed: 15389488]

Abbreviations used in this paper

LED	light-emitting diode
CMOS	complementary metal oxide semiconductor
ASIC	application-specific integrated circuit
CCD	charge-coupled device

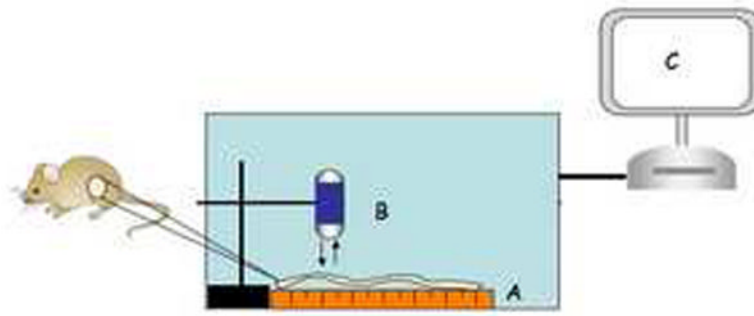


Figure 1. Light-tight chamber setup for white light imaging
Apparatus includes a moving platform controlled by a stepper motor (A), conventional CE (B) suspended above the platform, and data analysis system (C).

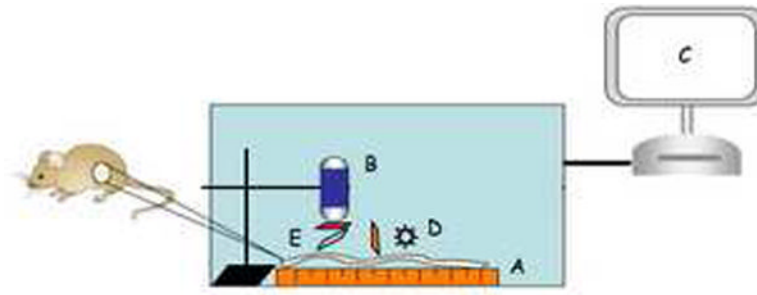


Figure 2. Light-tight chamber setup for NIRF imaging

Similar setup as in white light imaging (A – C) except for an external LED light source (D) and a filter set (E) suspended in between VCE and platform. The filter set consists of three filters: excitation filter (680 nm) vertical to the platform, dichroic filter at 45 degrees, and emission filter (700 nm) horizontal to the platform.

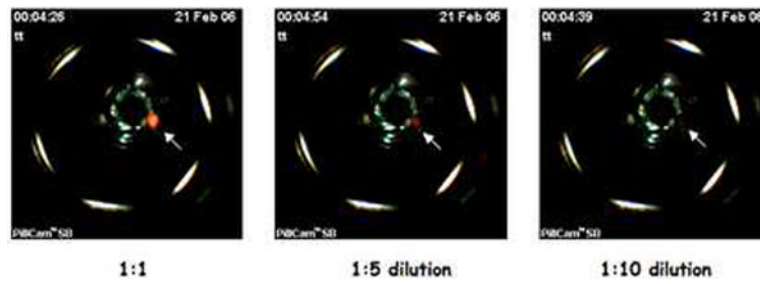


Figure 3. NIRF imaging of activated Prosense™ 680 at different concentrations
NIRF images of different dilutions of activated Prosense™ 680 over a ten fold concentration difference collected by modified CE. Note the progressive decrease in signal intensity with decreasing concentrations of activated probe.



Figure 4. CE based white light imaging of adenomatous polyps through custom built light-tight chamber

White light image by conventional CE of a segment of *Apc*^{Min/+} mouse colon containing two polyps (arrows).

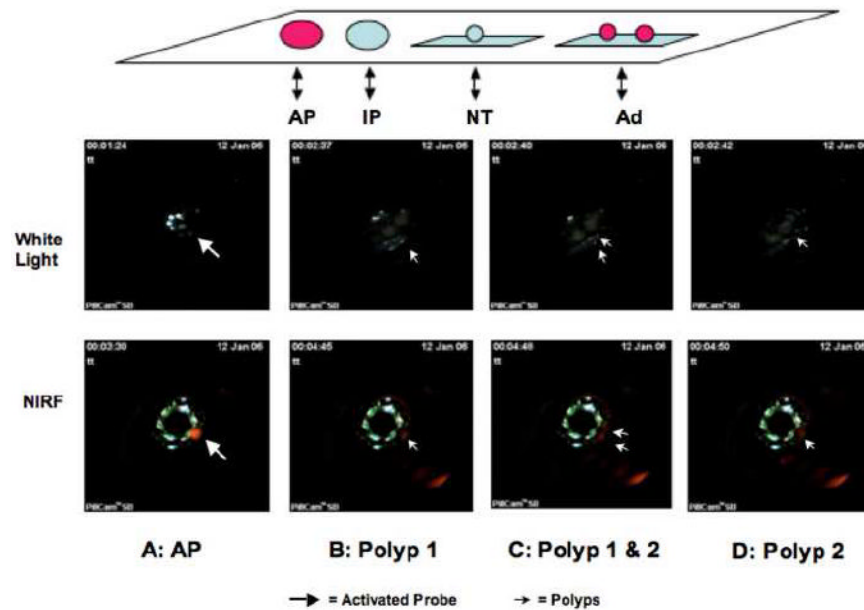
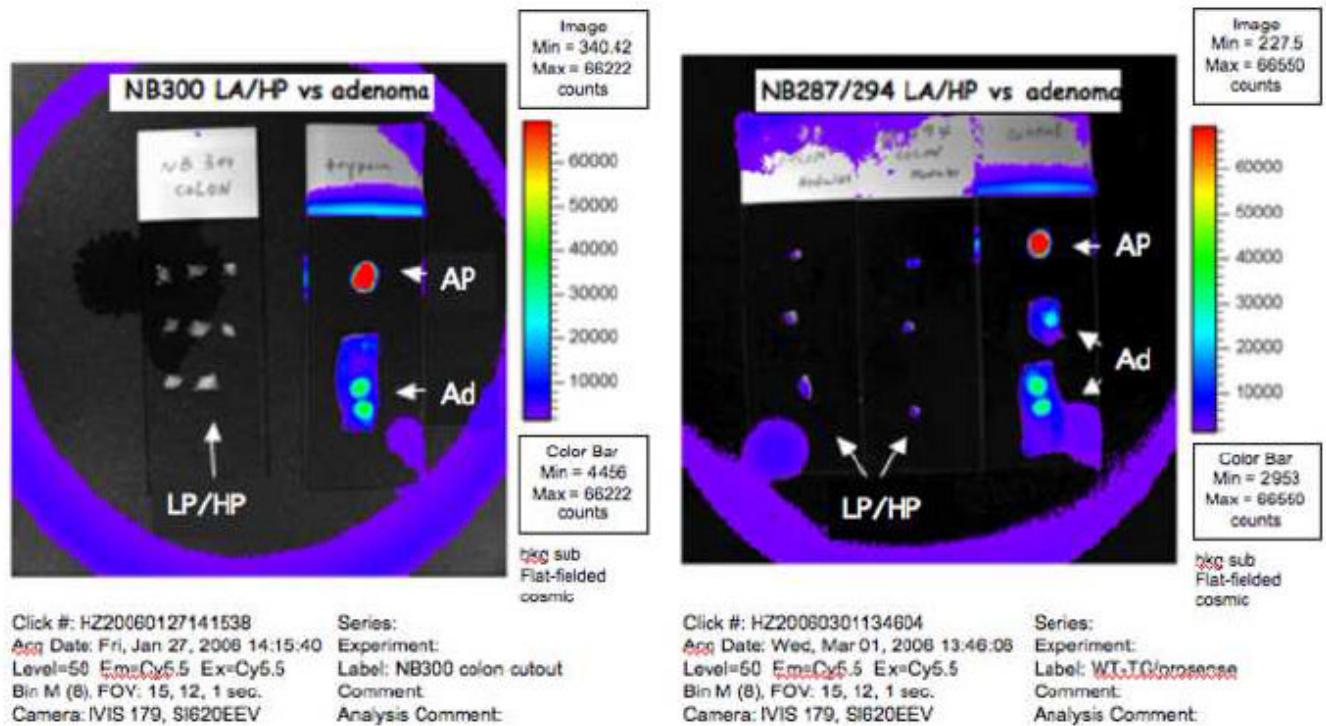
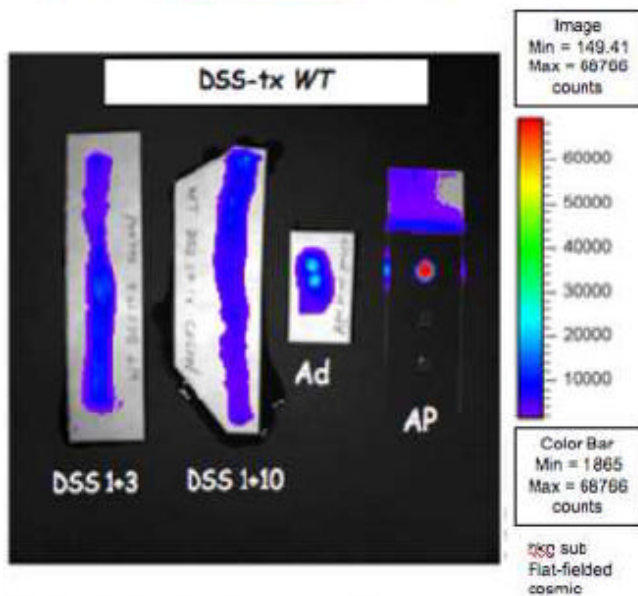


Figure 5.

Top Panel: Sample layout during typical white light and NIRF imaging with CE (top panel). Schematic illustration of sample layout in the order from left to right: AP = activated Prosense™ 680 as positive control; IP = negative inactive Prosense™ 680 as negative control; 3) NT= negative tissue control from uninjected animals; Ad = adenomatous polyps dissected from *Apc^{Min/+}* mouse colon. **Middle and Bottom Panels: CE based white light and NIRF images of activated probe (AP) and two adenomatous polyps (Ad).** The four panels show first the visualization of the activated probe (AP, block arrow) followed by images of two adenomatous polyps as they move into the view of the CE with polyp 1 visualized first (single solid arrow), both polyps 1 & 2 (double solid arrow) and then only polyp 2 (single solid arrow). The time when the AP probe is first visible serves as a reference for other frames which show images of the polyps under white light or NIRF. Note that the time elapsed between visualization of AP and visualization of polyps is almost identical with white light and NIRF imaging.

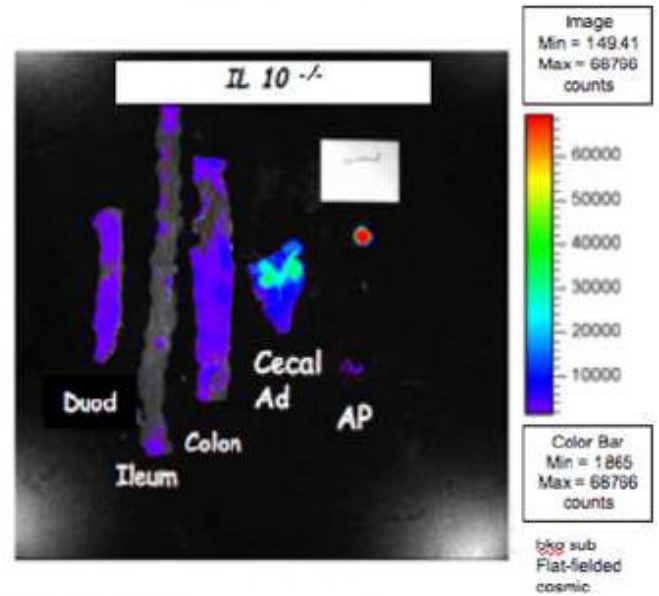
SOCS2-HT/GH-TG LP/HP vs *Apc*^{Min/+} AdenomaGH-TG LP/HP vs *Apc*^{Min/+} Adenoma**Figure 6. NIRF imaging of lymphoid polyps (LP) and hyperplastic polyps (HP)**

NIRF images collected by a Xenogen IVIS system of dissected colonic lymphoid polyps (LP) and hyperplastic polyps (HP) from mouse NB300, a *SOCS2-HT/GH-TG* (Right) and mice NB287 and NB294, which were *GH-TG* (left). Note the isolated lymphoid and hyperplastic polyps had no NIRF signal. Activated Prosense™ 680 (AP) and adenomatous polyps (Ad) from Prosense™ 680 injected *Apc*^{Min/+} mouse colon imaged under identical conditions served as positive controls.

DSS WT vs *Apc*^{Min/+} Adenoma

Click #: HZ20060203121012
 Acq Date: Fri, Feb 03, 2006 12:10:14
 Level=50 Em=Cy5.5 Ex=Cy5.5
 Bin M (8), FOV: 15, 12, 1 sec.
 Camera: IVIS 179, S1620EEV

Series:
 Experiment:
 Label: WT DSS1 + 3/1 + 10/prosense
 Comment:
 Analysis Comment:

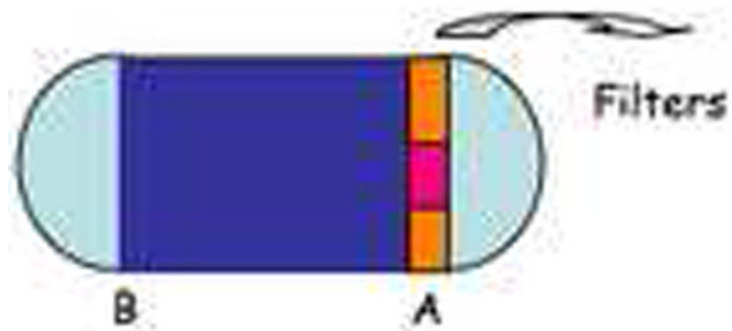
IL 10^{-/-} vs AP

Click #: HZ20060301141651
 Acq Date: Wed, Mar 01, 2006 14:16:53
 Level=50 Em=Cy5.5 Ex=Cy5.5
 Bin M (8), FOV: 15, 12, 1 sec.
 Camera: IVIS 179, S1620EEV

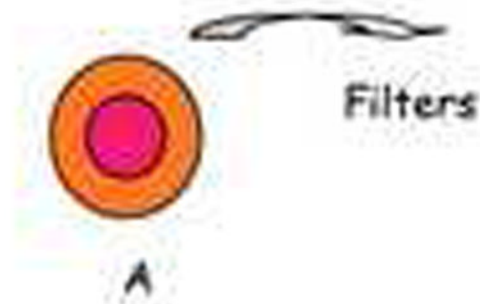
Series:
 Experiment:
 Label: IL 10 KO M3/prosense
 Comment:
 Analysis Comment:

Figure 7. NIRF imaging of acute and chronic intestinal inflammation

NIRF images captured by a Xenogen IVIS system of: Right = colon of DSS treated WT mice sacrificed 3 (DSS+3) or 10 days (DSS+10) after DSS treatment. Left = NIRF images of duodenum, ileum, colon and cecum of an IL-10^{-/-} mouse. Note background signals except for what proved to be a cecal adenoma (Cecal Ad). The inflamed colon had no NIRF signals. Activated ProsenseTM 680 (AP) served as positive control.



Longitudinal view



Cross-sectional view

Figure 8. Proposed design of integrated VCE with molecular imaging capability

Conversion of one of the twin camera CE into a NIRF imaging device by attaching a round planar filter to camera A, in front of the lens and illuminating LEDs. This round planar filter will be woven so that the center core covering the lens contains the emission filter and the outer donut-shaped rim covering the illuminating LEDs contains the excitation filter. The white light camera B of the CE remains intact at the other end of the capsule.